

Excitation Signal Design for THz Channel Sounding and Propagation Parameter Estimation

Jonas Gedschold^{*†}, Sebastian Semper^{*}, Michael Döbereiner[†], Reiner S. Thomä^{*}

^{*}Institute for Information Technology, TU Ilmenau, Helmholtzplatz 2, 98693 Ilmenau, Germany

[†]Fraunhofer Institute for Integrated Circuits (IIS), Am Vogelherd 90, Ilmenau, Germany

[‡]jonas.gedschold@tu-ilmenau.de

Abstract—In this publication, we analyze how the performance of propagation parameter estimation for THz channel sounding can be improved by the power spectrum design of a multicarrier waveform. To this end, we discuss the Fisher information of the propagation parameters and the corresponding deterministic Cramér-Rao lower bound (CRB) as well as their relation to the carrier powers of the excitation signal. We use these quantities to design waveforms that improve range estimation. In practice, optimizing the power spectrum requires prior knowledge of the propagation scenario which is usually not available. Hence, we propose two solutions which we compare numerically to the classical approach of equal power distribution. The numerical evaluation shows that an optimized power distribution can improve the CRB comparable up to a 4 dB gain in SNR depending on whether knowledge about the scenario can be acquired in advance with an additional measurement.

Index Terms—excitation signal design, channel sounding, high-resolution parameter estimation, terahertz

I. INTRODUCTION

Terahertz (THz) frequency bands promise—amongst others—high peak data rates for future mobile communication technologies [1], [2]. One of the research challenges is the constraint on received power due to shrinking effective antenna apertures at THz frequencies compared to sub-6 or mm-wave channels. An increase in transmit power to compensate for the path loss is limited by the capabilities of the THz amplifiers and can generate nonlinear distortions at the transmitter. Hence, one solution is to use high-gain antennas with small half-power beam widths to direct the transmit power to the receiver or to scan the environment for its multipath propagation properties. Additionally, THz frequency bands readily enable deployment of bandwidths of several GHz and the broadband transmit signals provide degrees of freedom to optimize the sending waveforms that are still in line with the power requirements.

In this publication, we focus on channel sounding, i.e., the measurement of the structure of the propagation channel to estimate meaningful propagation parameters such as time-of-flight of different propagation paths. Thus, we discuss waveform optimization according to criteria important for sounding. Considering the parameter estimation task, one of the available approaches is to maximize the information about the propagation parameters in the measurement. Ultimately, this decreases the variance of the estimation results [3], [4].

The signal optimization can be split up into two intertwined problems [5, Ch. 4]. On the one hand, the peak-to-average power

ratio (PAPR) should be minimal such that the amplifier can be operated closely to the upper end of its linear region. On the other hand, the power spectrum should be adjusted to concentrate the power on parts in the spectrum that are most informative for the task at hand. Multicarrier (or multisine) sounding signals are beneficial for both problems. Their generation by choosing the Fourier coefficients of the carriers allows a direct influence on the power spectrum. Furthermore, the relation between the phase distribution of the carriers and the PAPR of the waveform is well-investigated [6].

We begin this publication with a recap of general design procedures for multicarrier signals (Section II) and the considered parametric model (Section III). The contribution of this publication is a discussion on power spectrum design by analyzing the Fisher information of the propagation parameters and their relation to the carrier powers (Section IV). We substantiate this discussion with numerical examples (Section V).

A. Notation

Let $\mathcal{R}\{y\}$ be the real part of a complex number and y^* its conjugate. $\mathbf{E}(z)$ denotes the expected value of a random variable. Furthermore, we want to make use of a simplified Einstein notation which conveniently decouples the mathematical formulation from its implementation via vector/tensor products [7]. Say we want to calculate a tensor product between $\mathbf{a} \in \mathbb{C}^{K \times N \times I}$ and $\mathbf{b} \in \mathbb{C}^{N \times K \times J}$ to yield the result $\mathbf{c} \in \mathbb{C}^{I \times J}$. The elements of \mathbf{c} are defined as

$$\mathbf{c}_{i,j} = \sum_k \sum_n \mathbf{a}_{k,n,i} \cdot \mathbf{b}_{n,k,j}. \quad (1)$$

Instead of (1) we refer to the whole tensor \mathbf{c} with

$$\mathbf{c}_{i,j} = \mathbf{a}_{k,n,i} \cdot \mathbf{b}_{n,k,j}. \quad (2)$$

Hence, \mathbf{a} and \mathbf{b} are multiplied elementwise over those axes denoted with the same indices while the summation happens over those axes, whose index is present on the right-hand side but not on the left-hand side of the equation.

II. MULTICARRIER SOUNDING WAVEFORMS

Multicarrier signals are typically defined in the frequency domain using the discrete Fourier transform (DFT) notation

$$\mathbf{s}_n = \mathbf{c}_f \cdot \exp\left(j2\pi \frac{\mathbf{f}_f n}{N}\right) \quad (3)$$

with discrete frequencies

$$\mathbf{f}_f = -\frac{N}{2} + f \quad (4)$$

and $f, n = 0, \dots, N-1$. Each frequency bin represents a carrier with a total number of N , $\mathbf{s} \in \mathbb{C}^N$ is the discrete time domain waveform, and $\mathbf{c} \in \mathbb{C}^N$ the vector of carrier weights. Each carrier weight can be represented by $\mathbf{c}_f = \beta_f \cdot \exp(j\zeta_f)$ with $\beta_f = |\mathbf{c}_f|$ and $\zeta_f = \angle \mathbf{c}_f$. Hence, power and phase spectra can be designed independently. We start with the phase design.

A. Phase spectrum optimization

The phase spectrum directly determines the amplitude probability density function (PDF) of the time domain waveform and, hence, the PAPR. Phase designs for a minimal PAPR are well studied. We want to consider the solution from Schroeder [6] which is calculated as

$$\zeta_f = \zeta_0 - 2\pi \sum_{j=0}^{f-1} (f-j) \frac{\beta_j^2}{\|\beta\|^2}. \quad (5)$$

It considers the relative power of the carriers and provides a phase design for arbitrary power spectra. Additionally, one could apply further phase optimization such as iterative clipping which we will not discuss in this publication. The time domain waveform and the PDF are visualized for a flat power spectrum in Figure 1 (a-c).

We are now going to discuss the power spectrum design.

B. Power spectrum optimization

As motivated in the introduction, we want to design the power spectrum in a way that the variance of the parameter estimates is minimized under the constraint of limited transmit power. This variance is lower bounded by the Cramér-Rao bound (CRB) which corresponds to the main diagonal-elements of the inverse of the Fisher information matrix (FIM) $\mathbf{F} \in \mathbb{R}^{N_p \times N_p}$. Here, N_p denotes the number of model parameters. Given a parameter vector $\theta \in \mathbb{R}^{N_p}$, the variance of the parameter estimates (considering an unbiased estimator) is lower bounded as

$$\mathbf{E} \left(\hat{\theta}_i - \theta_i \right)^2 \geq (\mathbf{F}^{-1})_{ii}, \quad (6)$$

where the estimate is denoted by $\hat{\cdot}$ and $i = 1, \dots, N_p$. To solve the minimization problem, a scalar criterion is required that considers all parameters simultaneously. Hence, the problem of minimizing the individual variances can be replaced by maximizing the determinant of the FIM [8] which results in a minimized CRB for the estimator's variance.

In our case, we want to perform the maximization with respect to the carrier powers β_f^2 . For this, the response dispersion function is introduced [3] via

$$\nu_f(\beta) = \text{trace} \left([\mathbf{F}(\beta)]^{-1} \mathbf{F}(\tilde{\beta}_f) \right). \quad (7)$$

The FIM for a given set of carrier weights is represented by $\mathbf{F}(\beta)$. Furthermore, $\mathbf{F}(\tilde{\beta}_f)$ is evaluated for a single carrier input with power $\tilde{\beta}_f^2 = 1$ given that the full set of carrier weights is normalized to $\|\beta\|^2 = 1$. Hence, it compares the information of

the current power spectrum to concentrating all power on a single carrier.

An optimal design can now be found by the following iterative algorithm [8]:

Algorithm 1 Iterative FIM optimization

- 1: Start with uniform power distribution $\beta_f^{(0)} \leftarrow 1/\sqrt{N}$
 - 2: **while** $\max(\nu(\beta^{(k)})) - N_p > \epsilon$ **do**
 - 3: $\beta_f^{(k+1)} \leftarrow \nu_f(\beta^{(k)}) \cdot \beta_f^{(k)} / N_p$
 - 4: $k \leftarrow k + 1$
 - 5: **end while**
-

It has been shown that each iteration monotonically improves the power spectrum design, and as a consequence, the optimized power spectrum yields a lower CRB. Finally, to conduct an actual physical measurement, both phase and power spectra need to be brought together to generate the desired signal waveform. If the phase optimization for different power spectra results in different PAPRs the comparison of the resulting CRBs is unfair since a signal with a lower PAPR can be amplified more. Hence, the CRB needs to be modified according to the different PAPRs by normalization. This ensures that the signals are compared for the same peak values [5, Ch. 4].

Figure 1 (d-f) visualizes an optimized power spectrum for estimating the parameters of a propagation channel. To understand the resulting shape of the power spectrum we first need to introduce the model and the corresponding FIM in the following section.

III. DEVICE AND PROPAGATION MODEL

Perspectively, we want to analyze full multiple-input-multiple-output (MIMO) channel sounding at THz frequencies. Hence, we define the sampled observation of the radio channel by a 4-way vector $\mathbf{y} \in \mathbb{C}^{N_{tx} \times N_{rx} \times N_f \times N_t}$ with the number of transmit antennas N_{tx} , the number of receive antennas N_{rx} , the number of frequency samples N_f and the number of time samples N_t . We model the observation as $\mathbf{y} = \mathbf{m}(\theta) + \mathbf{n}$ with a deterministic model \mathbf{m} parameterized by vector θ and additive noise \mathbf{n} . The deterministic model can be split up into a propagation and a device model. The propagation model decomposes the channel into N_p specular propagation paths while the device model accounts for antenna beam patterns and the signal waveform.

The parameters of interest for each propagation path are direction of departure (DoD) and direction of arrival (DoA) represented by elevation and azimuth angles $\vartheta \in \mathbb{R}^{2 \times N_p}$ in a spherical coordinate system. Furthermore, a propagation delay $\tau \in \mathbb{R}^{N_p}$, a Doppler shift $\alpha \in \mathbb{R}^{N_p}$, as well as the real and imaginary part of a complex path weight $\gamma = [\gamma^r, \gamma^i] \in \mathbb{R}^{2 \times N_p}$ are considered. The path weights are usually defined as fully polarimetric which we omit for simplicity as the current discussion generalizes in a straightforward fashion to this case. Hence, the resulting parameter vector reads as

$$\theta = [\vartheta^{\text{dod}}, \vartheta^{\text{doa}}, \tau, \alpha, \gamma] \in \mathbb{R}^{8 \times N_p}. \quad (8)$$

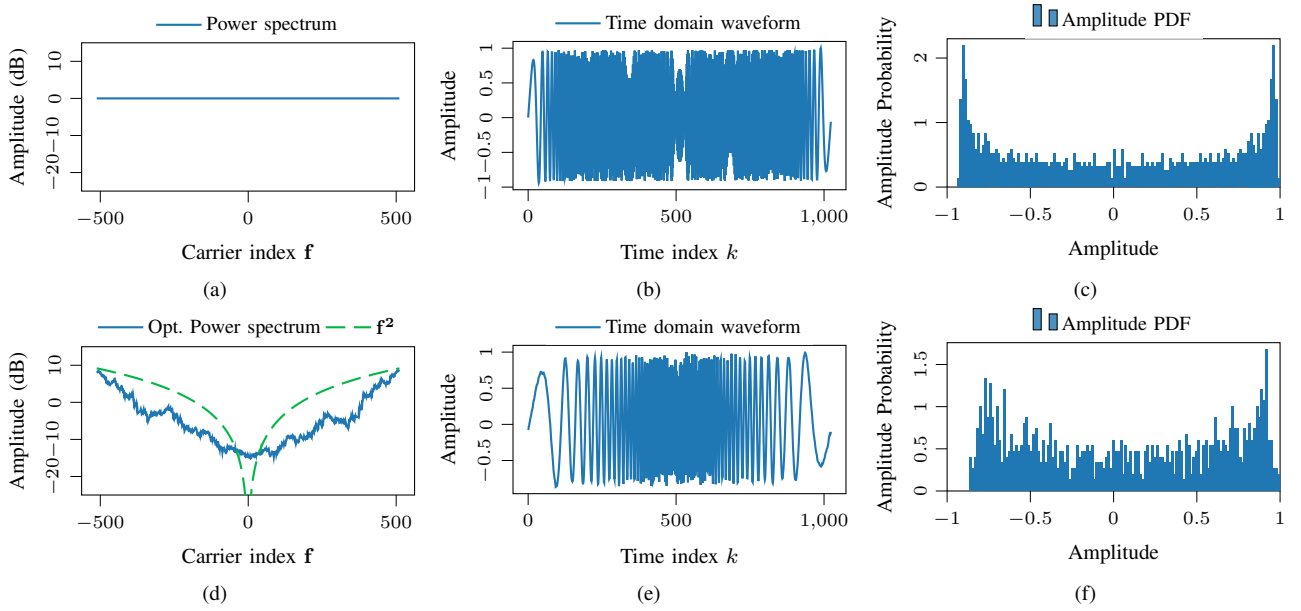


Fig. 1. Comparison of two waveforms with a flat (a-c) and an optimized (d-f) power spectrum.

We continue with defining the deterministic model \mathbf{m} .

A. Propagation Model

Considering the frequency response of a shift operation we define the so-called atomic model for the propagation delay as $\mathbf{a}^\tau : [0, 1) \rightarrow \mathbb{C}^{N_f}$

$$\mathbf{a}_f^\tau(\tau) = \exp(-j2\pi\mathbf{f}\tau) \quad (9)$$

and the atomic model for the Doppler shift as $\mathbf{a}^\alpha : [-1/2, 1/2) \rightarrow \mathbb{C}^{N_t}$

$$\mathbf{a}_t^\alpha(\alpha) = \exp(j2\pi\mathbf{t}\alpha) \quad (10)$$

given the discrete time instances $\mathbf{t} = [0, \dots, N_t - 1]$.

Using the atomic model components from above, the propagation part of the model can be defined as

$$\mathbf{p}_{f,t}(\boldsymbol{\tau}, \boldsymbol{\alpha}, \boldsymbol{\gamma}) = (\boldsymbol{\gamma}_p^r + j\boldsymbol{\gamma}_p^i) \cdot \mathbf{a}_f^\tau(\boldsymbol{\tau}_p) \cdot \mathbf{a}_t^\alpha(\boldsymbol{\alpha}_p) \quad (11)$$

which represents an outer product between the frequency and time atomic functions as well as a summation over the individual propagation paths.

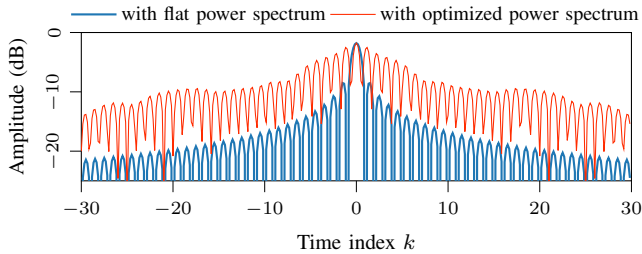


Fig. 2. Autocorrelation function for the two signals of Figure 1.

B. Device Model

For the device model, we assume that we can evaluate the frequency response of each transmitting and receiving antenna at arbitrary angles $\boldsymbol{\vartheta}$ with the functions

$$\mathbf{a}^{\text{tx}}(\boldsymbol{\vartheta}) \in \mathbb{C}^{N_f \times N_{\text{tx}}} \quad \text{and} \quad \mathbf{a}^{\text{rx}}(\boldsymbol{\vartheta}) \in \mathbb{C}^{N_f \times N_{\text{rx}}} \quad (12)$$

which can be represented, e.g., by the effective aperture distribution function (EADF) [7], [9], [10, Ch. 2.4.3].

Typically, the device model is agnostic of the actual signal waveform and assumes that the received signal is an observation of the band-limited impulse response of the channel. This is achieved by a matched filter correlation processing prior to parameter estimation. However, the matched filter response is degraded for the optimized excitation signals (see Figure 2). Hence, the parameter estimation is deteriorating due to model mismatch [11] unless the sounding signal waveform is accounted for in the model. We assume that the receiver is adjusted to the period length of the waveform such that each frequency sample represents an individual carrier. Thus, the carrier weights \mathbf{c} are added to the model. Summarizing, our device model reads as

$$\mathbf{d}_{tx,rx,f}(\mathbf{c}, \boldsymbol{\vartheta}^{\text{dod}}, \boldsymbol{\vartheta}^{\text{doa}}) = \mathbf{c}_f \cdot \mathbf{a}_{tx,f}^{\text{tx}}(\boldsymbol{\vartheta}_p^{\text{dod}}) \cdot \mathbf{a}_{rx,f}^{\text{rx}}(\boldsymbol{\vartheta}_p^{\text{doa}}) \quad (13)$$

and the full model \mathbf{m} results in

$$\mathbf{m}_{tx,rx,f,t}(\boldsymbol{\theta}) = \mathbf{p}_{f,t}(\boldsymbol{\tau}, \boldsymbol{\alpha}, \boldsymbol{\gamma}) \cdot \mathbf{d}_{tx,rx,f}(\mathbf{c}, \boldsymbol{\vartheta}^{\text{dod}}, \boldsymbol{\vartheta}^{\text{doa}}). \quad (14)$$

Now, we are ready to look at the Fisher information given the model \mathbf{m} and assumptions about the measurement noise \mathbf{n} .

C. Fisher Information

To calculate the Fisher information for the presented model, we first need to introduce the log-likelihood function λ rating the likelihood that a certain set of parameters belongs

to the observation \mathbf{y} . This completes the model from a statistical perspective since we assume a certain statistic for the measurement noise. We model the noise process \mathbf{n} as complex Gaussian noise with zero mean and covariance \mathbf{R} and we define

$$\lambda(\boldsymbol{\theta}|\mathbf{y}) = \ln(|\mathbf{R}|) + \mathbf{r}_{\mathbf{n}_1}^*(\boldsymbol{\theta}) \cdot \mathbf{R}_{\mathbf{n}_1, \mathbf{n}_2}^{-1} \cdot \mathbf{r}_{\mathbf{n}_2}(\boldsymbol{\theta}) \quad (15)$$

where we use $\mathbf{n}_{1,2}$ as shortcut for the indices (tx, rx, f, t) to denote the measurement dimensions. The residual \mathbf{r} given a set of parameters $\boldsymbol{\theta}$ is

$$\mathbf{r}(\boldsymbol{\theta}) = \mathbf{y} - \mathbf{m}(\boldsymbol{\theta}) \quad (16)$$

The Fisher information is the covariance of the score function at the maximum likelihood estimate which is the partial derivative of the log-likelihood function (15) with respect to the model parameters [12]. The formula for the elements of $\mathbf{F} \in \mathbb{R}^{(8 \cdot N_p) \times (8 \cdot N_p)}$ has been already derived for the presented models within the context of the parameter estimator RIMAX [10, Ch. 4.1.1] (or alternatively PyMAX [7]) and is

$$\mathbf{F}_{p_1, p_2}(\boldsymbol{\theta}) = 2 \cdot \mathcal{R} \left\{ \left(\frac{\partial}{\partial \boldsymbol{\theta}_{p_1}} \mathbf{m}_{\mathbf{n}_1}(\boldsymbol{\theta}) \right)^* \cdot \mathbf{R}_{\mathbf{n}_1, \mathbf{n}_2}^{-1} \cdot \frac{\partial}{\partial \boldsymbol{\theta}_{p_2}} \mathbf{m}_{\mathbf{n}_2}(\boldsymbol{\theta}) \right\}. \quad (17)$$

Interestingly, (17) does not depend on the observation \mathbf{y} but only on the model \mathbf{m} and the noise covariance. This allows us to perform the power spectrum optimization with Algorithm 1 without the need for measurements in between. We can directly evaluate the model derivatives in (17) for different carrier weights \mathbf{c} . What is required, though, is a prior knowledge of $\boldsymbol{\theta}$ to evaluate the derivatives at the appropriate values. We discuss two possible approaches in Section V. For ease of discussion, we are going to consider $\mathbf{R} = \sigma^2 \cdot \mathbf{I}$ with identity tensor \mathbf{I} corresponding to an i.i.d. circular Gaussian noise process with noise power σ^2 .

In the next section, we are going to analyze the frequency spectrum of \mathbf{F} which helps to understand the result of the power spectrum optimization.

IV. SPECTRUM OF THE FISHER INFORMATION

The determinant maximization with Algorithm 1 considers all model parameters simultaneously. However, not all parameters can be influenced by the power spectrum in an equal way. Intuitively, the information about the model parameters has to depend on frequency such that it will be influenced by altering the power spectrum. This is only the case for the delay and antenna parts of the model. The antennas can be considered to have an angle-dependent transfer function that strongly depends on the antenna design. This will be analyzed in the further course of the project. In this publication, we are going to focus on the delay parameters.

The partial derivatives of \mathbf{m} with respect to $\boldsymbol{\tau}$ read as

$$\frac{\partial}{\partial \boldsymbol{\tau}_p} \mathbf{m}_{tx, rx, f, t}(\boldsymbol{\theta}) = (\gamma_p^r + j\gamma_p^i) \cdot \overbrace{(-j2\pi\mathbf{f}_f)}^{\text{inner}} \cdot \overbrace{\mathbf{a}_f^T(\boldsymbol{\tau}_p)}^{\text{outer}} \cdot \mathbf{a}_t^\alpha(\boldsymbol{\alpha}_p) \cdot \mathbf{d}_{tx, rx, f}(\mathbf{c}, \boldsymbol{\vartheta}_p^{\text{dod}}, \boldsymbol{\vartheta}_p^{\text{doa}}), \quad (18)$$

where the inner and outer derivative of the delay atom (9) are marked accordingly. Due to the structure of \mathbf{m} as a sum over the individual propagation paths, the derivative only depends on the part of the model belonging to a single propagation path indexed by p .

To evaluate the frequency spectrum of \mathbf{F} , we evaluate (17) while omitting the summation over the frequency index f in the tensor product. This corresponds to the property, that \mathbf{F} is additive over the individual samples of the observation [4]. We can now calculate the spectrum for an individual delay parameter (which resides on the main diagonal of \mathbf{F}) as

$$\mathbf{F}_{\boldsymbol{\tau}_p, \boldsymbol{\tau}_p, f} = \frac{2 \cdot |\gamma_p|^2}{\sigma^2} \cdot (2\pi\mathbf{f}_f)^2 \cdot N_t \cdot |\mathbf{c}_f|^2 \cdot \left| \mathbf{a}_{tx, f}^{\text{tx}}(\boldsymbol{\vartheta}_p^{\text{dod}}, \boldsymbol{\varphi}_p^{\text{dod}}) \right|^2 \cdot \left| \mathbf{a}_{rx, f}^{\text{rx}}(\boldsymbol{\vartheta}_p^{\text{doa}}, \boldsymbol{\varphi}_p^{\text{doa}}) \right|^2. \quad (19)$$

It depends on the signal-to-noise-ratio (SNR) of the propagation path determined by $|\gamma_p|^2$ and σ^2 , a factor N_t from the summation over the time axis, the carrier power, and factors determined by the directivity of the antenna elements in direction of the corresponding angles. Most interestingly, there is a strong frequency-dependent factor $(2\pi\mathbf{f}_f)^2$ originating from the inner derivative of the delay atom. Hence, $\mathbf{F}_{\boldsymbol{\tau}_p, \boldsymbol{\tau}_p, f}$ has a general \mathbf{f}^2 -shaped spectrum weighted by the transfer functions of the antennas and the power spectrum of the signal.

In the next section, we are going to analyze the improvement of the CRB when designing the power spectrum in two different ways.

V. NUMERICAL EXAMPLE

Since our model equations are nonlinear, the calculations of the derivatives and the FIM require a knowledge of the propagation parameters. Those are—of course—unknown otherwise no sounding would be necessary. We propose two possible solutions which we analyze numerically in this section:

- 1) Since the values of the FIM for the delay parameters (19) do not depend on the actual delay parameters of the paths, we can define an \mathbf{f}^2 -shaped power spectrum to improve the CRB for delay estimation.
- 2) We start with *blind probing* using a flat power spectrum to achieve prior knowledge about the propagation scenario. After initial parameter estimation, we optimize the power spectrum using the parameter estimates and rerun the measurement to refine the estimation (which requires a static scenario).

We calculate the CRB for a single-input-single-output model with omnidirectional antennas (thus omitting the antenna-related terms) with $N_f = 1024$ and $N_t = 16$. The path parameters $\boldsymbol{\tau}, \boldsymbol{\alpha}$ as well as the magnitude and phase of γ are drawn independently from uniform distributions for a total number of 25 propagation paths. Additionally, we averaged the results over 10 different sets of parameters and the propagation paths resulting in a single CRB value for each model component.

Figure 3 compares the delay CRB for 3 different power spectra over a varying noise power level σ^2 . The noise level is calculated relative to the upper limit on path powers. *Flat* refers

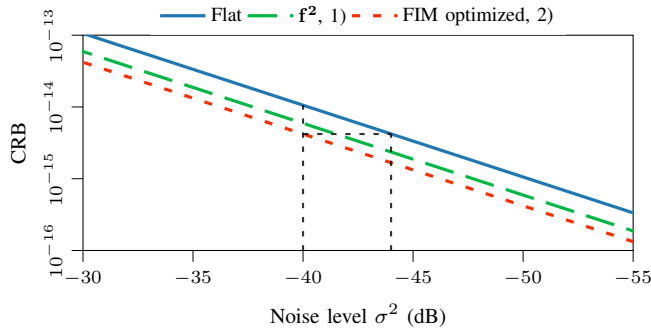


Fig. 3. CRB comparison of a flat power spectrum, an f^2 -shaped power spectrum and a spectrum resulting from iterative FIM optimization.

to a power spectrum with equal power distribution, f^2 to solution 1) and *FIM optimized* to solution 2). The resulting CRBs are compensated for the PAPR of the time domain waveforms.

In the case of solution 2), we simulated the process of performing a *blind measurement* prior to spectrum optimization. Thus, we generated the observation y for a flat power spectrum by using the model equations and performed a parameter estimation using the PyMAX estimator [7]. Using the estimation results, we optimized the power spectrum with Algorithm 1. Afterwards, we calculated the CRB for this power spectrum.

A direct comparison of the three power spectra is visualized in Figure 1 (a) and (d). *Opt. Power spectrum* refers to solution 2) and f^2 to solution 1). The time domain waveform and amplitude PDF in (e) and (f) belong to the optimized spectrum. Both spectra follow the same trend with concentrating power at the edges of the spectrum to improve the information about the delay parameters while showing a symmetry due to the symmetric definition of the delay atom (9).

Back to Figure 3, both solutions provide a lower CRB for delay estimation compared to the flat power spectrum while the FIM optimization performs slightly better than the f^2 spectrum. The black dotted line highlights, that the power spectrum optimization reaches the same CRB as the flat power spectrum with a ≈ 4 dB higher SNR.

Not shown in this figure is the fact, that the CRB for the Doppler parameters does not change over the different power spectra as expected.

VI. DISCUSSION

The numerical evaluation in Section V shows that the theoretical lower bound for the variance of propagation delay estimates can be improved by power spectrum optimization. The improvement can especially be useful for applications concerning THz frequencies with stricter transmit power constraints. FIM-based optimization tailors the power spectrum to the actual propagation scenario. This, however, requires prior knowledge about the channel which could be achieved by a prior measurement. In this way, measurement and computation time rise and the channel would be constrained to be static within one optimization run. Ultimately, it has to be analyzed how accurate the prior parameter estimate has to be to allow

a certain improvement of the CRB. Alternatively, a slightly lower improvement of the CRB can already be achieved by an f^2 -shaped power spectrum without scenario-specific optimization.

Since the CRB only represents a theoretical lower bound for any unbiased estimator, it remains to analyze, how the actual implementation of an estimator has to be adapted such that it can reach the CRB with such excitation signals. The robustness of the initialization routine as well as the conditioning of the FIM play an important role. It also remains to analyze, how antennas would influence the power spectrum design and if angle estimation could be improved by an optimized spectrum.

The presented power spectra in this publication also raise the idea of considering sparse excitation signals where only a few carriers at the edges of the bandwidth are occupied. This could be especially interesting for applications like *Integrated Communication and Sensing* where distant spectral resource blocks can be combined for high-resolution delay estimation with a huge bandwidth.

ACKNOWLEDGMENT

This work is partly sponsored by the *Deutsche Forschungsgesellschaft (DFG)* under research projects *Metrologie für die THz Kommunikation* (FOR 2863) and JCRS CoMP with Grant-No. TH 494/35 – 1 (504990291), as well as by the Federal Ministry for Economic Affairs and Climate Action of Germany in the project DOCT (Grant-No. 1922001H).

REFERENCES

- [1] C. Han, Y. Wang, Y. Li, Y. Chen, N. A. Abbasi, T. Kürner, and A. F. Molisch, "Terahertz wireless channels: A holistic survey on measurement, modeling, and analysis," *IEEE Communications Surveys & Tutorials*, no. 3, 2022.
- [2] T. Eichler and R. Ziegler, "White paper: Fundamentals of thz technology for 6g," Rohde & Schwarz, Tech. Rep., 2023.
- [3] "Chapter 6 experiment design," in *Dynamic System Identification*, ser. Mathematics in Science and Engineering, G. C. Goodwin and R. L. Payne, Eds., Elsevier, 1977.
- [4] G. Jávorszky, S. Boyd, I. Kollár, L. Vandenbergh, and S. Wu, "Optimal excitation signal design for frequency domain system identification using semidefinite programming," 1996.
- [5] R. Pintelon and J. Schoukens, *System Identification, A Frequency Domain Approach*. John Wiley & Sons, 4, 2012.
- [6] M. Schroeder, "Synthesis of low-peak-factor signals and binary sequences with low autocorrelation (corresp.)," *IEEE Transactions on Information Theory*, no. 1, 1970.
- [7] S. Semper, M. Döbereiner, C. Steinmetz, M. Landmann, and R. S. Thomä, "High resolution parameter estimation for wideband radio channel sounding," *IEEE Transactions on Antennas and Propagation*, 2023.
- [8] E. Van den Eijnde and J. Schoukens, "On the design of optimal excitation signals," *IFAC Proceedings Volumes*, no. 3, 1991, 9th IFAC/IFORS Symposium on Identification and System Parameter Estimation 1991, Budapest, Hungary, 8-12 July 1991.
- [9] M. Landmann and G. Del Galdo, "Efficient antenna description for mimo channel modelling and estimation," in *7th European Conference on Wireless Technology*, 2004., 2004.
- [10] A. Richter Dr. - Ing., "Estimation of radio channel parameters," de, Ph.D. dissertation, Technische Universität Ilmenau, 2005.
- [11] M. Landmann, M. Kaske, and R. S. Thoma, "Impact of incomplete and inaccurate data models on high resolution parameter estimation in multidimensional channel sounding," *IEEE Trans. Antennas Propag.*, no. 2, 2012.
- [12] L. L. Scharf and C. Demeure, *Statistical signal processing : detection, estimation, and time series analysis*. 1, 1991.